JOC Article

erythro-1-Naphthyl-1-(2-piperidyl)methanol: Synthesis, Resolution, NMR Relative Configuration, and VCD Absolute Configuration

A. Solladié-Cavallo,*[,†] C. Marsol,[†] M. Yaakoub,[†] K. Azyat,[†] A. Klein,[†] M. Roje,[†] C. Suteu,[‡] T. B. Freedman,*[,§] X. Cao,[§] and L. A. Nafie*[,§]

Laboratoire de Stéréochimie Organométallique, ECPM/Université Louis Pasteur, 67087 Strasbourg, France, Chiral Technologies Europe, 67404 Illkirch, France, and Department of Chemistry, Syracuse University, Syracuse, New York 13244-4100

cavallo@chimie.u-strasbg.fr; lnafie@syr.edu; tbfreedm@syr.edu

Received April 29, 2003

The *erythro* isomer of 1-naphthyl-1-(2-piperidyl)methanol **4**, an efficient chiral modifier for asymmetric heterogeneous hydrogenation, was obtained as the major isomer (95%) in two steps while the *threo* isomer can be obtained as the major isomer (67%) in three steps. *erythro*-**4** and *threo*-**4** were resolved on a CHIRALCEL OD-RH column. It has been shown by VCD that the diastereomer determined as the *erythro* by NMR was indeed the *erythro* and that the first eluted (−)-enantiomer on CHIRALCEL OD-R or -RH columns has the (1*R*,2*S*) configuration. The VCD studies identify the presence of at least five conformers in $CDCl_3$ solution. Moreover, this (−)-(1*R*,2*S*) absolute configuration found by VCD is consistent with the expected stereo-outcome of catalytic hydrogenation of pyruvate into lactate, which supported the (+)-(1*S*,2*R*) assignment.

Introduction

Various chiral amino alcohols **1**[1] and arylamines **2**[2,3] have been tested for the asymmetric heterogeneous hydrogenation of α-keto esters over supported platinum catalysts, but cinchonidine **3**[4] has proven to be the best inducer of chirality until now. Therefore, the synthesis of amino alcohol **4**, having two vicinal asymmetric carbons similar to those found in cinchonidine, was envisaged and happened to be an efficient modifier.[5]

We report here (i) two synthetic routes toward amino alcohol **4** leading either to the *threo* or to the *erythro* isomer preferentially; (ii) determination of the relative *threo* or *erythro* configuration (using ^{1}H NMR); (iii) chromatographic resolution of both *threo* and *erythro* isomers (using chiral columns); and (iv) determination of the absolute configuration of the (−)-*erythro* by using vibrational circular dichroism (VCD).[6−9]

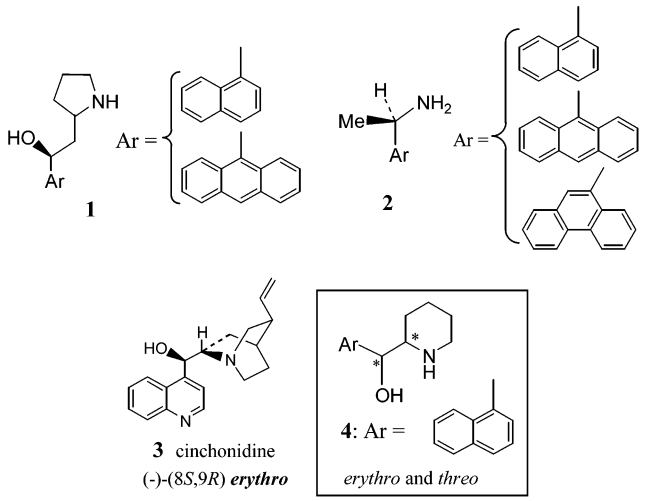

Results and Discussion

Synthesis from Formamidine 5 (*Threo* Isomer = Major). Amino alcohol **4** was synthesized in a two-step

† ECPM/Université Louis Pasteur.
‡ Chiral Technologies Europe.
§ Syracuse University.

(1) Minder, B.; Schuerch, M.; Mallat, T.; Baiker, A.; Heinz, T.; Pfaltz, A. *J. Catal.* **1996**, 160, 261−268.
(2) Heinz, T.; Wang, G.; Pfaltz, A.; Minder, B.; Schuerch, M.; Malat, T.; Baiker, A. *J. Chem. Soc., Chem. Commun.* **1995**, 1421.
(3) Solladie-Cavallo, A.; Marsol, C.; Suteu, C.; Garin, F. *Enantiomer* **2001**, *6*, 245−249.
(4) Blaser, H. U.; Jalett, H. P.; Wiehl, J. *J. Mol. Catal.* **1991**, *68*, 215−220.
(5) Solladie-Cavallo, A.; Marsol, C.; Garin, F. *Tetrahedron Lett.* **2002**, *43*, 4733−4735.
(6) Nafie, L. A.; Freedman, T. B. In *Infrared and Raman Spectroscopy of Biological Materials*; Yan, B., Gremlish, H. U., Eds.; Marcel Dekker: New York, 2001; Vol. 24, pp 15−54.
(7) Nafie, L. A.; Freedman, T. B. In *Circular Dichroism*: *Principles and Applications*, 2nd ed.; Nakanishi, K., Berova, N., Woody, R. W., Eds.; Wiley: New York, 2000; pp 97−131.
(8) Polavarapu, P. L.; Zhao, C. *Fresenius' J. Anal. Chem.* **2000**, *366*, 727−734.
(9) Stephens, P. J.; Devlin, F. J. *Chirality* **2000**, *12*, 172−179.
(10) Nafie, L. A. *Appl. Spectrosc.* **2000**, *54*, 1634−1645.
(11) Frisch, M. J.; Trucks, G. W.; Schlegel, H. B.; Scuseria, G. E.; Robb, M. A.; Cheeseman, J. R.; Zakrzewski, V. G.; Montgomery, J. A. Jr.; Stratmann, R. E.; Burant, J. C.; Dapprich, S.; Millam, J. M.; Daniels, A. D.; Kudin, K. N.; Strain, M. C.; Farkas, O.; Tomasi, J.; Barone, V.; Cossi, M.; Cammi, R.; Mennucci, B.; Pomelli, C.; Adamo, C.; Clifford, S.; Ochterski, J.; Petersson, G. A.; Ayala, P. Y.; Cui, Q.; Morokuma, K.; Malick, D. K.; Rabuck, A. D.; Raghavachari, K.; Foresman, J. B.; Cioslowski, J.; Ortiz, J. V.; Stefanov, B. B.; Liu, G.; Liashenko, A.; Piskorz, P.; Komaromi, I.; Gomperts, R.; Martin, R. L.; Fox, D. J.; Keith, T.; Al-Laham, M. A.; Peng, C. Y.; Nanayakkara, A.; Gonzalez, C.; Challacombe, M.; Gill, P. M. W.; Johnson, B.; Chen, W.; Wong, M. W.; Andres, J. L.; Gonzalez, C.; Head-Gordon, M.; Replogle, E. S.; Pople, J. A. *Gaussian 98*; A.9 Ed.; Gaussian, Inc.: Pittsburgh, PA, 1998.

10.1021/jo0345502 CCC: $25.00
Published on Web 08/21/2003

SCHEME 1

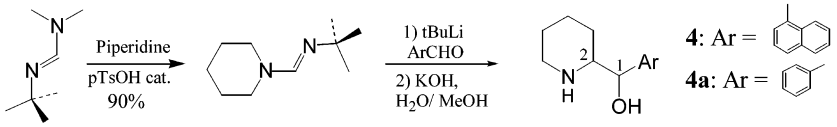

SCHEME 2

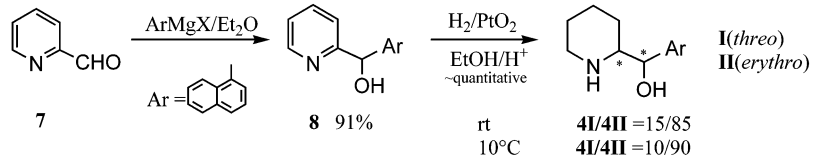

TABLE 1. Amino Alcohols 4 and 4a from Condensation of ArCHO onto the Lithium Derivative of Formamidine 5

ArCHO	product	yield (%)	I/II	δ H_1I[a]	$^3J_{12}$[b]	δ H_1II[a]	$^3J_{12}$[b]
1-naphthaldehyde	**4**	70	67/33	5.24	6	5.44	4
benzaldehyde	**4a**	60	69/31	4.36	7.5	4.56	5

[a] NMR (200 MHz in $CDCl_3$) in ppm. [b] NMR (200 MHz in $CDCl_3$) in Hz.

but one-pot procedure from formamidine **5** (Scheme 1) which has been prepared from *N*,*N*-dimethylformamidine **6** following the usual Meyers procedures.[14,15] The results are presented in Table 1.

The condensation of the lithiated anion of **5** with the desired aldehyde provided **4** in 70% yield. Since the *threo*/*erythro* configurations of **4a** diastereomers were known,[16,17] this compound was also prepared in the same way, through condensation of the same lithiated anion with benzaldehyde (60% yield). The desired amino alcohols **4** and **4a** were obtained as mixtures of the two possible diastereomers **I** and **II**, and the **I**/**II** ratios have been determined using proton H_1 doublets which appear between 4.2 and 5.6 ppm (Table 1). It appeared that diastereomer **I**, characterized by the most shielded H_1 doublet and the largest $^3J_{12}$, was major in both cases.

Synthesis from 2-Pyridinecarboxaldehyde 7 (*Erythro* Isomer = Major). Amino alcohol **4** has also been obtained in two steps and higher yield from commercially available 2-pyridinecarboxaldehyde **7**, Scheme 2, but with an inverted diastereoselectivity compared to the previous synthesis from formamidine; diastereomer **II** characterized by the most deshielded H_1 doublet and by the smallest $^3J_{12}$ was now major (85−90%).

The condensation of the naphthyl Grignard on aldehyde **7** proceeded in high yield providing the naphthylpyridyl alcohol **8**, and PtO_2 hydrogenation of **8** in EtOH/HCl (1 equiv) was quantitative after 6 h.

***Erythro/Threo* Configuration by NMR.** The *erythro* and/or *threo* structures of **4a** have already been assigned,[16,17] and the $^3J_{12}$ values are 5 and 7.5 Hz, respectively.

TABLE 2. Relative Configuration of Vicinal Amino Alcohols by ^{1}H NMR in $CDCl_3$

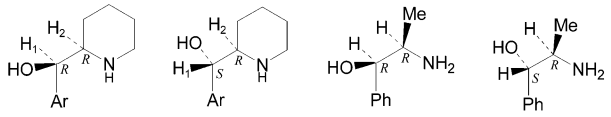

compd	$^3J_{1-2}$ (Hz)	Δ^3J (Hz)	configuration
4I (67%)	6.0	2	threo
4II (33%)	4.0		erythro
4aI (69%)	7.5	2.5	*threo* (known)
4aII (31%)	5.0		*erythro* (known)
(1*S*,2*S*)-pseudoephedrine	8	4	*threo* (known)
(1*R*,2*S*)-ephedrine	4		*erythro* (known)
(1*S*,2*S*)-Me-pseudoephedrine	9.5	5.5	*threo* (known)
(1*R*,2*S*)-Me-ephedrine	4		*erythor* (known)

For amino alcohols having similar CH(OH)−CH(NH) systems and of known relative configuration such as *erythro*-ephedrine, *threo*-pseudoephedrine, methylated *erythro*-ephedrine, and methylated *threo*-pseudoephedrine,[18] it has been also observed that the values of $^3J_{12}$ coupling constants were larger in the *threo* isomers than in the *erythro* isomers (Table 2). Although the difference between ^3J-*erythro* and ^3J-*threo* is smaller for compound **4a** (Δ^3J = 2.5 Hz) than for ephedrines (Δ^3J = 4 Hz, 5.5 Hz), the trend is identical with ^3J-*erythro* < ^3J-*threo*.

Since compounds **4** and **4a** differ only by the size of the aryl group, it can reasonably be postulated that isomer *threo*-**4** will also exhibit the largest value of $^3J_{12}$ as does compound **4a**, and thus, the *threo* configuration was assigned to diastereomers **4I**, Table 2.

The differences between ^3J-*erythro* and ^3J-*threo* for compounds **4** is small and almost identical (∼2 Hz) to that of **4a**, but further NMR studies of a 85/15 *erythro*−*threo* mixture of amino alcohol **4** in various solvents, Table 3, showed that this difference Δ^3J ($^3J_{12}$ *threo* − $^3J_{12}$-*erythro*) becomes larger and more significant in C_6D_6 and CD_3OD (and without inversion: that is, the same isomer (15%) retains the largest value for the coupling constant).

One can thus reasonably assign the *threo* configuration to diastereomer **4I** having the largest $^3J_{12}$ value and the most shielded H_1 doublet.

(12) Stephens, P. J. *J. Phys. Chem.* **1985**, *89*, 748−52.
(13) Cheeseman, J. R.; Frisch, M. J.; Devlin, F. J.; Stephens, P. J. *Chem. Phys. Lett.* **1996**, *252*, 211−220.
(14) Meyers, A. I.; Ten Hoeve, W. *J. Am. Chem. Soc.* **1980**, *102*, 7125−7126.
(15) Meyers, A. I.; Edwards, P. D.; Rieker, W. F.; Bailey, T. R. *J. Am. Chem. Soc.* **1984**, *106*, 3270−3276.
(16) LaPidus, J. B.; Fauley, J. J. *J. Org. Chem.* **1971**, *36*, 3065−3067.
(17) Meyers, A. L.; Edwards, P. D.; Bailey, T. R.; Jagdmann, G. E. Jr. *J. Org. Chem.* **1985**, *50*, 1019−1026.
(18) van der Zeijden, A. A. H. *Tetrahedron*: *Asymmetry* **1995**, *6*, 913−918.

TABLE 3. ^{1}H NMR (400 MHz): $^3J_{12}$ of a 85/15 *Erythro*−*Threo* Mixture of Compound 4 in Various Solvents

solvent	*erythro* major (Hz)	*threo* minor (Hz)	Δ^3J (Hz)
C_6D_6	3	6.5	3.5
CD_3OD	4.5	8.5	4
$CDCl_3/CD_3OD$[a]	4.5	7	2.5
$CDCl_3$	3.5	5.5	2

[a] $^3J_{12}$ *threo* = 8.2 Hz, $^3J_{12}$ *erythro* = 4.8 Hz have been found in the same solvent mixture[19]

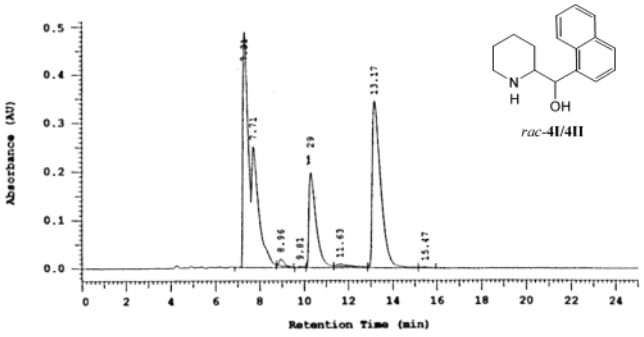

FIGURE 1. Chromatogram of the resolution of the four isomers of amino alcohol **4** on a CHIRALCEL OD-RH.

Resolution of a 67% *Threo*/33% *Erythro* Mixture of 4. Analytical separation of the racemic mixture of amino alcohol **4** (67-*threo*/33-*erythro* diastereomeric ratio) was performed on a CHIRALCEL OD-RH (150 × 4.6 mm, 5 μM) with acetonitrile/ ethanolamine 100:0.1 as mobile phase (flow rate = 0.5 mL/min, *T* 25 °C, DAD 235 nm and 0.02 mg injected). The chromatographic parameters are: $k'_1 = 1.03$, $k'_2 = 1.14$, $k'_3 = 1.86$, $k'_4 = 2.66$.

As reported in Figure 1, the first eluting enantiomers of diastereomer **I** (*major*, *threo*) and diastereomer **II** (*minor*, *erythro*) are overlapping, while the second eluting enantiomers of the corresponding diastereomers are well separated.

On a preparative scale, 344 mg of *rac*-**4I/4II** (2/1) were separated using a CHIRALCEL OD column (250 × 50 mm, 20 μm) and the same mobile phase (100 mL/min), with a total recovery of 92% of the starting product, in three fractions which after evaporation of the solvent and chiral analysis gave as follows:

150 mg (44%): mixture of enantiomer 1 of diastereomer **I** (**4I1**) and enantiomer 1 of diastereomer **II** (**4II1**): mixture **I/II** ∼ 2/1

52 mg (15%): enantiomer 2 of diastereomer **II** (**4II2**), ee = 100%, de = 99% (containing 0.5% of enantiomer 2 of diastereomer **I**, **4I2**)

114 mg (33%): enantiomer 2 of diastereomer **I** (**4I2**), ee = 100%, de = 96.4% (containing 1.8% of enantiomer 2 of diastereomer **II**, **4II2**)

After recrystallization from acetonitrile to completely remove ethanolamine, the specific rotations of enantiomers *threo*-**4I2** and *erythro*-**4II2** were determined:

$$\textit{erythro}\text{-}\mathbf{4II2}\text{: } [\alpha]_D = +82 \pm 1 \ (c = 0.43, CHCl_3)$$

$$\textit{threo}\text{-}\mathbf{4I2}\text{: } [\alpha]_D = +69 \pm 1 \ (c = 0.98, CHCl_3)$$

Resolution of a 5% *Threo*/95% *Erythro* Mixture of 4. Semipreparative separation of the racemic mixture of amino alcohol **4** (5 *threo*/95 *erythro* diastereomeric ratio) was performed again on a CHIRALCEL OD-R (250 × 8 mm, 7 μM) with acetonitrile/ethanolamine 100:0.1 as mobile phase (flow rate =2 mL/min, *T* 25°C, UV detection 235 nm). The chromatographic parameters are: $k'_1 = 0.81$, $k'_2 = 1.18$.

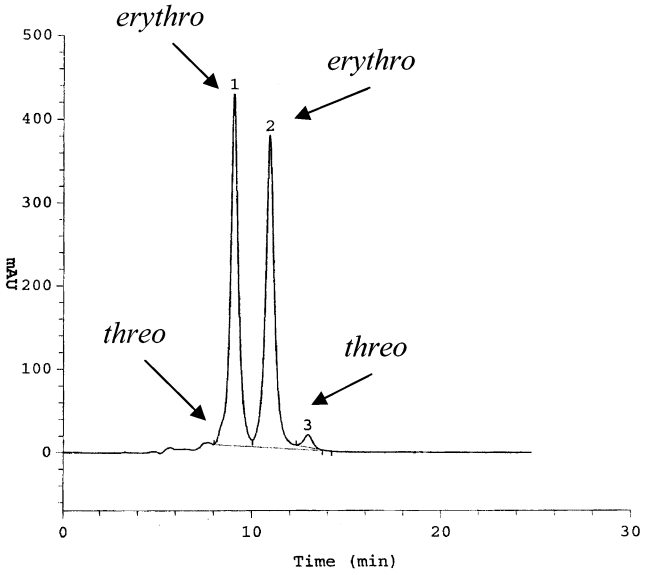

FIGURE 2. Chromatogram of the resolution of a 5/95 threo/erythro mixture of amino alcohol **4** on a CHIRALCEL OD-R.

The corresponding chromatogram shown in Figure 2 is comparable to the previous one, shown in Figure 1, with identical succession of isomers **4I1**−**4II1**−**4II2**−**4I2** but with an inversion of the diastereomers ratio (from **I/II** = 5/95 for Figure 2 to **I/II** = 67/33 for Figure 1).

As seen in Figure 2, the first eluting enantiomer of diastereomer **I** (minor (5%), *threo*) appears as a shoulder on the left of the peak of the first eluting enantiomer of diastereomer **II** (major (95%), *erythro*), in the third position comes the second eluting enantiomer of the *erythro* diastereomer (**II**) and finally (fourth position) the second enantiomer of the *threo* diastereomer (**I**). During this experiment enantiomer **1** of diastereomer **II**−*erythro* (**4II1**) was isolated pure, Figure 2, by collecting only the top of peak 2 and was used for VCD analysis. This sample **4II1** is the (−)-*erythro* as the **4II2**, which was isolated preparatively above, had a plus sign for the rotation ($[\alpha]_D = +82 \pm 1$ ($c = 0.43$, $CHCl_3$)).

Absolute Configuration of (−)-*erythro*-4II1 Using VCD. Vibrational circular dichroism (VCD) is a well-established method for determination of absolute configuration and solution conformation of chiral molecules.[6−9,20−25] The method entails comparison of observed IR and VCD spectra with spectra calculated at the DFT level for

(19) Delgado, A.; Mauleon, D.; Rosell, G.; Salas, M. L.; Najar, J. *An. Quim., Ser. C* **1987**, *83*, 90−95.
(20) Dyatkin, A. B.; Freedman, T. B.; Cao, X.; Dukor, R. K.; Maryanoff, B. E.; Maryanoff, C. A.; Matthews, J. M.; Shah, R. D.; Nafie, L. A. *Chirality* **2002**, *14*, 215−219.
(21) Freedman, T. B.; Dukor, R. K.; van Hoof, P. J. C. M.; Kellenbach, E. R.; Nafie, L. A. *Helv. Chim. Acta*. **2002**, *85*, 1160−1165.
(22) Freedman, T. B.; Cao, X.; Oliveira Regina, V.; Cass Quezia, B.; Nafie, L. A. *Chirality* **2003**, *15*, 196−200.
(23) Solladie-Cavallo, A.; Balaz, M.; Salisova, M.; Suteu, C.; Nafie, L. A.; Cao, X.; Freedman, T. B. *Tetrahedron: Asymmetry* **2001**, *12*, 2605−2611.

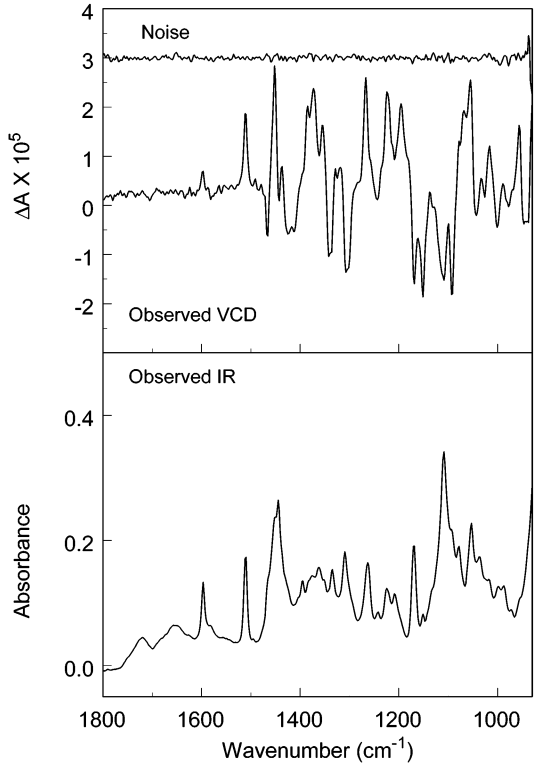

FIGURE 3. IR (lower frame) and VCD (upper frame) spectra of **4II1**, 11 mg/100 μL $CDCl_3$, 98 μm path length BaF_2 cell, 4 cm^{-1} resolution, 12 h collection for sample and solvent. Uppermost trace is the VCD noise. Solvent spectra have been subtracted.

conformers of a specified absolute configuration. Because solution conformers do not interchange on the vibrational time scale, calculated spectra for individual conformers can be summed to identify prevalent solution conformers in the sample.

IR and VCD spectra of (−)-*erythro*-**4II1**, Figure 3, were recorded in $CDCl_3$ as solvent. A mull was also prepared from the oily sample and it was observed that the spectra of the mull and the solution were nearly identical. An additional absorbance measurement was obtained in the hydrogen-stretching region for the same $CDCl_3$ solution, shown in Figure 4.

Calculations of optimized geometries, vibrational force fields, and IR and VCD intensities were carried out with Gaussian 98[11] at the DFT level with the B3LYP functional and 6-31G* basis set, for several conformations of the (1*R*,2*S*)-configuration of the *erythro* isomer.

Compound **4** in the (1*R*,2*S*)-configuration can assume three orientations of the O−C−C−N dihedral that result in stable structures **C1**, **C2**, and **C3** in Scheme 3. In addition, two 180° rotations of the naphthyl group, two chair conformations for the piperidyl group, and two positions for the NH hydrogen are possible for each structure **C1**, **C2**, and **C3**. Hydrogen bonding between the OH and NH groups is possible only for orientations **C1** and **C2**.

Low energy conformations within each orientation were identified and optimized at the DFT level. The lowest energy structures found for each orientation are shown in Figure 5.

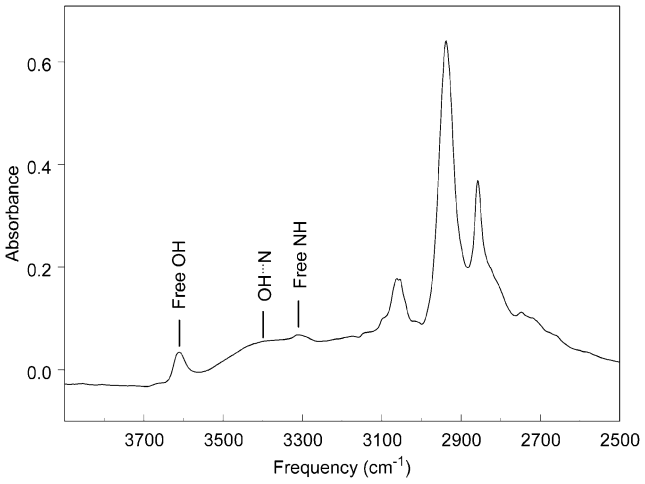

FIGURE 4. IR spectrum of **4II1** in the hydrogen-stretching region.

SCHEME 3. ***Erythro* (1*R*,2*S*) Conformations**

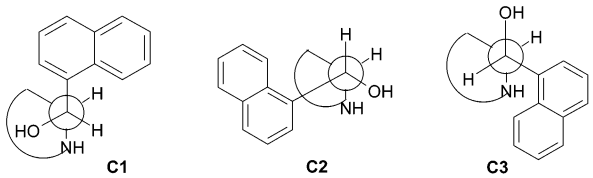

Conformer **C1a** (O−C−C−N dihedral = −54.06°) is stabilized by OH···N hydrogen bonding and has (*R*)-configuration at the nitrogen. In **C1b** (O−C−C−N dihedral = −66.58°), the configuration at N is *S*, and the hydrogen bonding is NH···O. In **C2a** (O−C−C−N dihedral = 51.52°, *S* at N), the hydrogen bonding is OH···N. The corresponding NH···O-bonded conformer is **C2b** (O−C−C−N dihedral = 55.64°, *R* at N). In Conformer **C3a**, with *trans* O−C−C−N (O−C−C−N dihedral = 169.34°, *R* at N), no intramolecular hydrogen-bonding is possible, but the NH and OH bonds are both stabilized by interaction with the aromatic π-system.

The orientation of the "free" OH bond is also stabilized by π-interaction in conformers **C1b** and **C2b**. Conformers without hydrogen bonding or π-stabilization are calculated at much higher energy as were structures with rotated naphthyl or inverted piperidyl chair. The energies shown in Figure 5 are relative to conformer **C1a**, and are for the gas-phase species. Such calculations tend to overestimate the stabilization of OH···N relative to NH···O hydrogen bonding. The calculated IR and VCD spectra for the five lowest energy *erythro* conformers are compared to experiment in Figure 6.

A number of features in the calculated spectrum of the lowest energy conformer, **C1a**, correlate with experiment. However, for many other experimental VCD and IR bands, there is no counterpart in the calculated spectrum of **C1a**. Although the calculated relative energies indicate that the other conformers would contribute less than 10%

(24) Solladie-Cavallo, A.; Sedy, O.; Salisova, M.; Biba, M.; Welch, C. J.; Nafie, L.; Freedman, T. *Tetrahedron*: *Asymmetry* **2001**, *12*, 2703−2707.

(25) Solladie-Cavallo, A.; Marsol, C.; Pescitelli, G.; Di Bari, L.; Salvadori, P.; Huang, X.; Fujioka, N.; Berova, N.; Cao, X.; Freedman, T. B.; Nafie, L. A. *Eur. J. Org. Chem*. **2002**, 1788−1796.

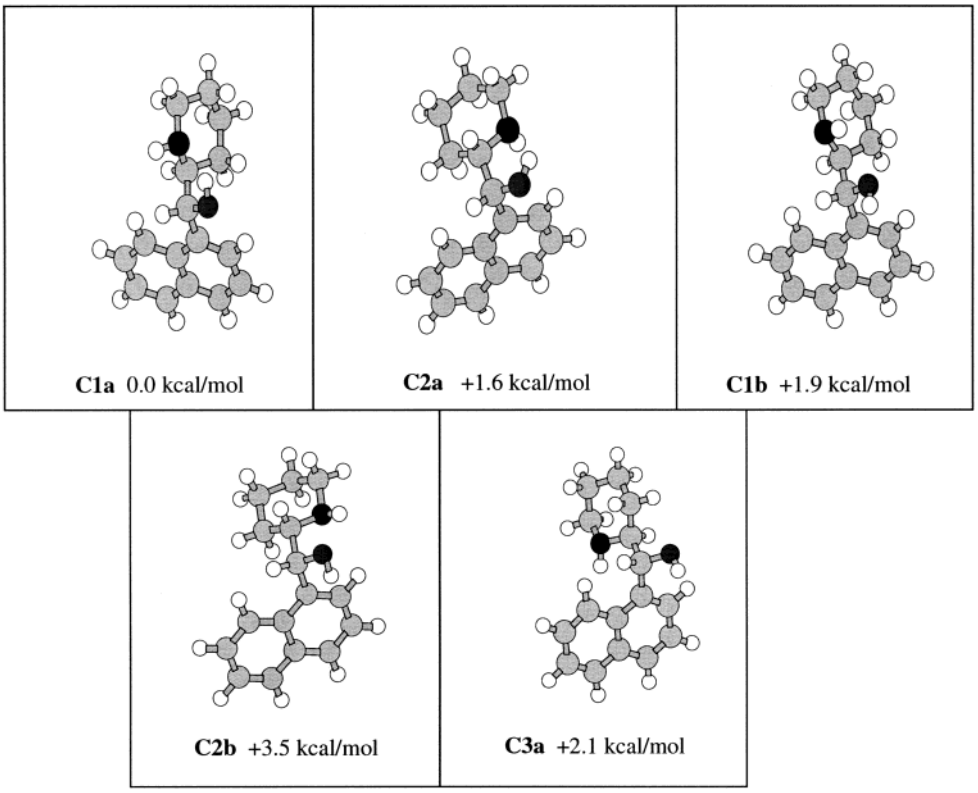

FIGURE 5. Optimized structures of the five lowest energy (1*R*,2*S*)-*erythro* conformations.

in the gas phase, the experimental IR spectrum in the OH/NH stretching region indicates the presence of free OH bonds for **4II1** in $CDCl_3$ solution (Figure 4). The complexity of the experimental IR and VCD spectra, compared to the calculated spectra of individual conformers, is also indicative of multiple conformations in the $CDCl_3$ solution. From Figure 6, calculated VCD features for each conformer can be distinguished that correlate with experimental features. Five such bands, one for each conformer, are identified in Figure 6. The positive band 1 (1452 cm^{-1}) correlates uniquely with conformer **C2a** (1422 cm^{-1}), assigned to C(1)−OH deformation and C(1)−H deformation. Band 2 (1435 cm^{-1}) corresponds to the intense negative VCD feature arising from the same motions in conformer **C2a** (1425 cm^{-1}). The negative band 3 (1091 cm^{-1}) is most prominent in conformer **C1b** (1082 cm^{-1}), arising from C−O stretch and piperidyl ring stretch. The intense positive VCD at 1054 cm^{-1} (band 4) correlates with a feature for conformer **C3a** (1063 cm^{-1}) due to C(1)−C(2) stretch, C−O stretch, C−OH deformation, and NH deformation. The positive VCD intensity for band 5 (956 cm^{-1}) is only observed for conformer **C2b** (944 cm^{-1}; C(1)−C(2) stretch, NH and OH deformations, and piperidyl ring stretch). Without additional information on the relative conformer populations, we consider first equal contributions for the five conformers calculated. The average spectra (equal weighting for each of the five conformers) are compared to experiment in Figure 7, where both observed and calculated spectra are plotted on the same molar absorptivity scales. This conformer weighting yields a much-improved fit with the experimental data, compared to conformer **C1a** alone.

The comparison in Figure 7 provides strong evidence that (−)-**4II1** has the (1*R*,2*S*)-configuration. Other weighting schemes or the addition of additional, higher energy conformations may possibly improve the fit, but based on the complexity of the spectra and the wide variation in VCD features as the conformation is changed, there is no quantitative basis for an alternate weighting scheme at this time.

To demonstrate that VCD can be used to distinguish between the *erythro* and *threo* diastereomers, we have also calculated VCD spectra for the (1*R*,2*R*)-configuration. The O−C−C−N rotamers of the (1*R*,2*R*)-*threo* configuration are shown in Scheme 4. Intramolecular hydrogen bonding is possible for **C1′** and **C2′**. The optimized structures of the five lowest energy *threo* conformations are shown in Figure 8.

The conformers are labeled for comparable O−C−C−N dihedral angle and hydrogen-bonding patterns relative to the *erthro* conformers: **C1′a** (O−C−C−N dihedral = −48.70°, *S* at N, OH−N); **C1′b** (O−C−C−N dihedral = −59.27°, *R* at N, NH−O); **C2′a** (O−C−C−N dihedral = 50.02°, *S* at N, OH−N); **C2′b** (O−C−C−N dihedral = 57.12°, *R* at N, NH−O); **C3′a** (O−C−C−N dihedral = −170.22°, no intramolecular hydrogen bonding, *S* at N) (Figure 9).

Compared to the *erythro* conformers, there is a wider range of energies and a different energy ordering of the conformers, which can be associated with unfavorable steric interactions involving the naphthyl group and nitrogen lone pair in **C2′b** and the naphthyl group and a piperidyl methylene hydrogen in **C3′a**.

The calculated spectra of the five *threo* conformers are compared to experiment in Figure 9, where the order of the spectra displayed allows direct correlation with the same hydrogen-bonding orientations as for the (1*R*,2*S*)-conformers in Figure 6.

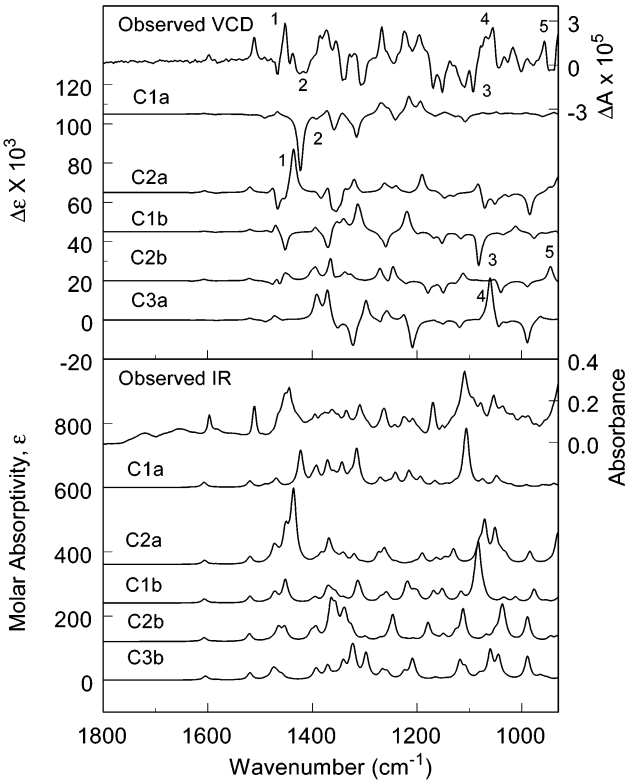

FIGURE 6. Comparison of IR (lower frame) and VCD (upper frame) spectra observed for **4II1** (right axes) with calculation for *erythro* (1*R*,2*S*)-conformers **C1a**, **C2a**, **C1b**, **C2b**, and **C3a** (left axes). Calculated spectra are offset along the intensity axis for clarity.

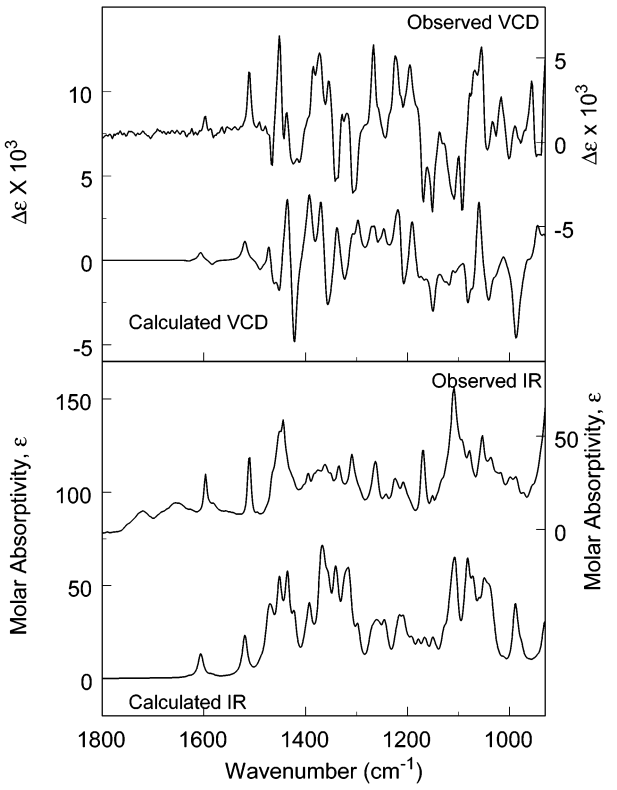

FIGURE 7. Comparison of IR (lower frame) and VCD (upper frame) spectra observed for **4II1** (right axes) with the average calculated spectra for (1*R*,2*S*)-conformers **C1a**, **C1b**, **C2a**, **C2b**, and **C3a** (left axes).

No distinct correlations are observed between the observed data and the calculated spectra for the lowest energy (1*R*,2*R*)-conformer **C2′a**. For the average spectra of the *threo* conformers, poor agreement with experiment is found for both the (1*R*,2*R*)- and (1*S*,2*S*) *threo* forms (Figure 10, plotted on the same molar absorptivity scales). In Figure 10, comparison of the observed spectra with the average calculated spectra for *erythro* (1*R*,2*S*)- and (1*S*,2*R*)- and *threo* (1*R*,2*R*)- and ((1*S*,2*S*)-configurations clearly demonstrates that agreement with the observed VCD spectrum is obtained only for the *erythro* (1*R*,2*S*)-configuration.

This study thus demonstrates the large differences in the VCD spectra expected for the diastereomers of 1-naphthyl-1-(2-piperidyl)methanol, and confirms the sample (−)-**4II1**, determined *erythro* by NMR, to be *erythro* and establishes the configuration of (−)-**4II1**-*erythro* as (1*R*,2*S*) with populations of three O−C−C−N rotamers and both OH···N and NH···O hydrogen bonding in $CDCl_3$ solution.

Conclusion

The *erythro* isomer of 1-naphthyl-1-(2-piperidyl)methanol **4**, an efficient chiral modifier for asymmetric heterogeneous hydrogenation, was easily obtained in two steps (via a naphthyl Grignard addition on 2-pyridaldehyde followed by a catalytic hydrogenation of the pyridyl ring) as the major isomer (95%) and then isolated pure via Et_2O crystallization. *erythro*-**4** and *threo*-**4** were resolved on a CHIRALCEL OD-RH column.

SCHEME 4. *Threo* (1*R*,2*R*) Conformations

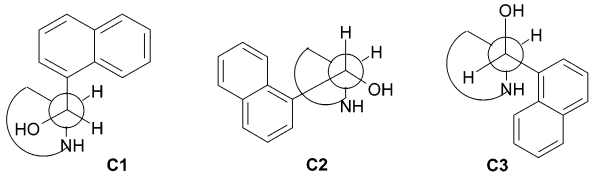

It has been shown by VCD that the diastereomer determined as the *erythro* by NMR was indeed the *erythro* and that the first eluted (−)-enantiomer on CHIRALCEL OD-R or RH columns has the (1*R*,2*S*) configuration. The VCD studies identify the presence of at least five conformers in $CDCl_3$ solution.

Moreover, this (−)-(1*R*,2*S*) absolute configuration found is consistent with the expected stereo-outcome of catalytic hydrogenation of pyruvate into lactate[5] which supported the (+)-(1*S*,2*R*) assignment. It was indeed observed[5] that (−)-(1*R*,2*S*)-*erythro*-cinchonidine provides the (*R*)-lactate while the (+)-*erythro*-**4** (**4II2**) provided the (*S*)-lactate.

Experimental Section

Synthesis from Formamidine 5. General Procedure. To a solution of piperidine formamidine **5** (2.0 g, 11.88 mmol, 1.0 equiv) in a ether/THF mixture (15/4 mL) was added (at −78 °C) *tert*-butyllithium 1.7 M (8.5 mL, 14.25 mmol, 1.2 equiv). The solution was stirred at −20 °C for 1 h resulting in formation of a white precipitate. The reaction mixture was cooled to −78 °C, the desired aldehyde (1.1 equiv) added, and the mixture slowly warmed to 0 °C over 5 h. The solution was poured into 30 mL of 10% HCl and extracted with ether (2 ×

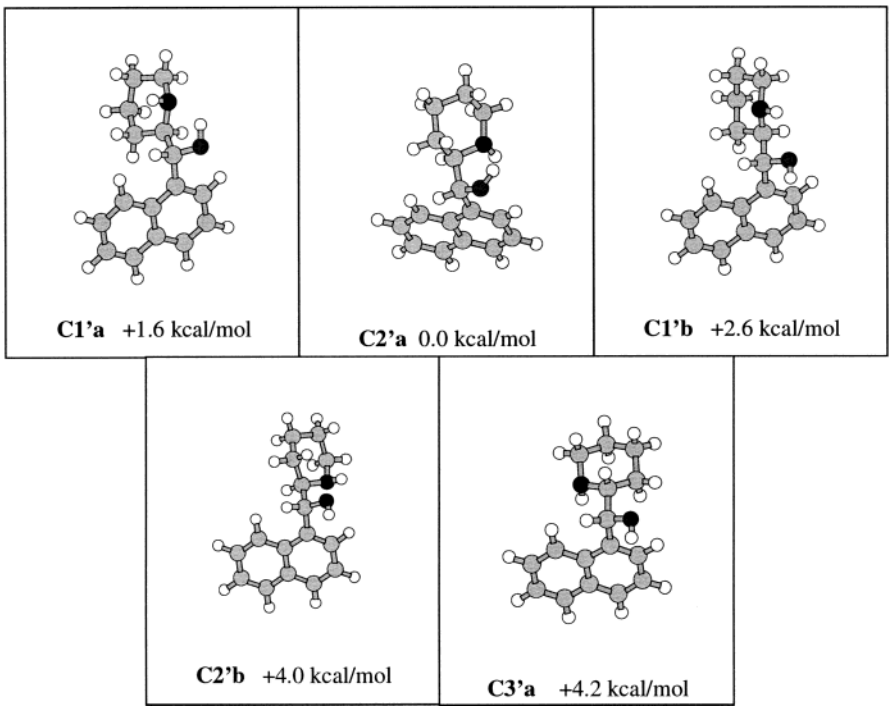

FIGURE 8. Optimized structures of the five lowest energy (1*R*,2*R*)-*threo* conformations.

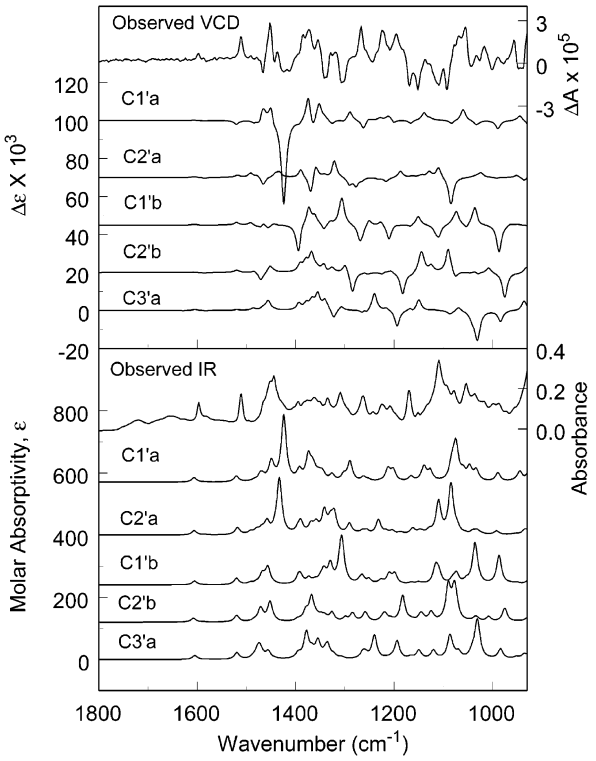

FIGURE 9. Comparison of IR (lower frame) and VCD (upper frame) spectra observed for **4II1** (right axes) with calculation for *threo* (1*R*,2*R*)-conformers **C1′a**, **C2′a**, **C1′b**, **C2′b**, and **C3′a** (left axes). Calculated spectra are offset along the intensity axis for clarity.

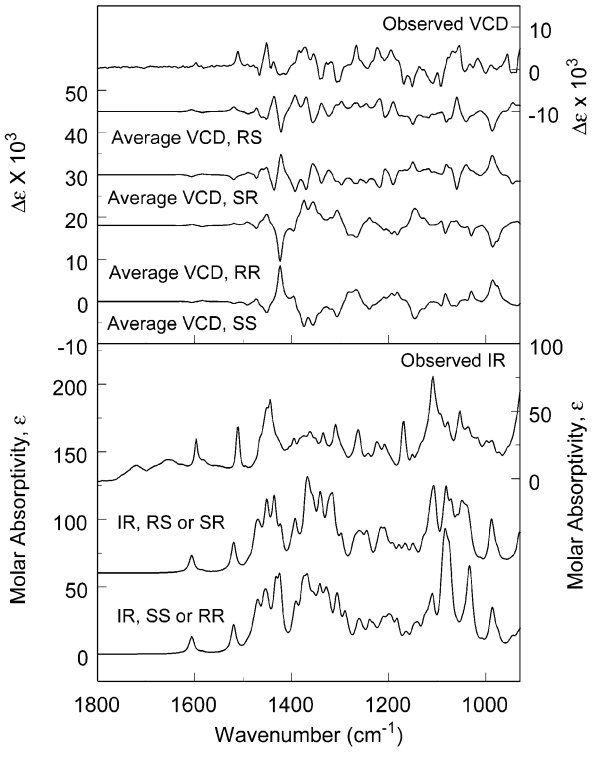

FIGURE 10. Comparison of IR (lower frame) and VCD (upper frame) spectra observed for **4II1** (right axes) with the average calculated spectra for *threo* conformers **C1′a**, **C1′b**, **C2′a**, **C2′b**, and **C3′a** in the (1*R*,2*R*)- and (1*S*,2*S*)-configurations and the average calculated spectra for *erythro* conformers **C1a**, **C1b**, **C2a**, **C2b**, and **C3a** in the (1*R*,2*S*)- and (1*S*,2*R*)-configurations (left axes). Calculated spectra offset on the intensity axes for clarity.

10 mL). The aqueous layer was then made basic (pH 12) with 20% NaOH and extracted several times with dichloromethane. The combined organic phases were concentrated under vacuum, and then a solution of the resulting crude product in 25 mL of MeOH, 4 mL of water, and 4 g of KOH was heated at 60 °C for 24 h. After cooling, the mixture was extracted with dichloromethane (5 × 15 mL). The combined dichloromethane

phases were dried over Na_2SO_4, the solvents were removed at reduced pressure, and the amino alcohol was isolated and purified by chromatography on silica gel (CH_2Cl_2/MeOH 4/1).

Synthesis from 2-Pyridinecarboxaldehyde 7. General Procedure for Naphthyl Grignard Addition. To a stirred suspension of activated magnesium turnings (123 mg, 5.06 mmol, 1.01 equiv) in anhydrous Et_2O (6 mL) were added successively a few drops of 1,2-dibromoethane and a solution of 1-bromonaphthalene (1.3 g, 5,06 mmol, 1.01 equiv) in anhydrous Et_2O (13 mL). The mixture was refluxed for 1 h and then cooled to room temperature, and a solution of 2-pyridyl aldehyde (0.54 g, 5 mmol, 1 equiv) in anhydrous Et_2O (18 mL) was added dropwise. There is an immediate precipitation, and the mixture was stirred overnight at room temperature. A saturated aqueous NH_4Cl solution (10 mL) and water (10 mL) were then added, followed by extraction with Et_2O. The joined organic phases were dried over anhydrous Na_2SO_4 and concentrated under vacuum. The crude product was purified by chromatography on silica gel (Et_2O/*n*-hexane 6/4) giving 1.07 g (91%) of **8**.

Hydrogenation. In a glass tube fitting perfectly inside a 100 mL autoclave were introduced a solution of **8** in ethanol (16 mL), concentrated hydrochloric acid (0.19 mL, 1 equiv), and PtO_2 (30 mg). Hydrogen was introduced and the solution maintained at 50 atm of pressure for 8 h while the autoclave was cooled at −10 °C. After the catalyst was filtered off, the solvent was evaporated under vacuum. The resulting solid was dissolved into water (5 mL), a 2 M NaOH solution (0.65 mL) was added, and the mixture was extracted with chloroform (3 × 20 mL). The joined organic phases were dried over anhydrous Na_2SO_4, and the solvent was evaporated. Amino alcohol **4** was obtained in quantitative yield as a mixture of *erythro*/*threo* 90/10 which gave the pure *erythro* isomer after crystallization from Et_2O (60%).

5: ^{1}H NMR (200 MHz, $CDCl_3$) δ 1.17 (9H, s), 1.54 (6H, m), 3.22 (4H, m), 7.27 (1H, s); ^{13}C NMR (50 MHz, $CDCl_3$) δ 25.0, 25.6, 31.3, 46.6, 151.0.

8: mp 88−91 °C; ^{1}H NMR ($CDCl_3$) δ 5.43 (1H, s, −O*H*), 6.44 (1H, s, −C*H*), 7.07 (1H, d, J = 7.7 Hz), 7.23 (1H, dd, J = 4.9 Hz, J = 2.3 Hz), 7.48 (4H, m), 7.57 (1H, td, J = J = 7.7 Hz, J = 1.7 Hz), 7.86 (2H, m) 8.13 (1H, m), 8.67 (1H, d, J = 4.3 Hz); ^{13}C NMR ($CDCl_3$) δ 73.6, 121.4, 122.5, 124.4, 125.3, 125.6, 126.2, 126.3, 128.7, 128.8, 131.3, 134.2, 136.9, 138.1, 147.9, 160.9.

4I-*threo*: ^{1}H NMR (400 MHz, $CDCl_3$) δ 1.15−1. 5 (5H, bm), 1.76 (1H, bd, H3e), 2.58 (1H, td, ^2J = 12 Hz, ^3J = 12, 3 Hz, H5a), 2.96 (1H, bdd, H1a), 3.07 (1H, bd, H5e), 5.24 (1H, d, J = 6 Hz, H1′), 7.50 (3H, m), 7.65 (1H, d, J = 7.0 Hz), 7.81 (1H, d, J = 7.0 Hz), 7.89 (1H, d, J = 7.0 Hz), 8.11 (1H, d, ^3J = 7 Hz); ^{13}C NMR (100 MHz, $CDCl_3$) δ 24.8, 26.4, 29.6, 46.8, 61.8, 74.2, 123.8, 124.5, 125.7, 125.9, 126.3, 128.4, 129.3, 131.3, 134.3, 138.6. **4II-*erythro***: mp 134−136 °C; ^{1}H NMR (400 MHz, $CDCl_3$) δ 1.15−1.65 (5H, m), 1.76 (1H, m), 2.67 (1H, td, ^2J = 12 Hz, ^3J = 12, 2 Hz, H5a), 3.07 (2H, m, H1a+H5e), 5.44 (1H, d, J = 4 Hz, H1′), 7.50 (3H, m), 7.75 (1H, d, J = 7 Hz), 7.81 (1H, d, J = 7 Hz), 7.89 (1H, d, J = 7 Hz), 8.11 (1H, d, J = 7 Hz); ^{13}C NMR (100 MHz, $CDCl_3$) δ 24.6, 26.5, 29.6, 47.3, 60.8, 73.9, 123.6, 124.7, 125.8, 125.9, 126.3, 128.2, 129.3, 131.3, 134.3, 138.6. **4I**/**4II** = 67/33: mp 50−52 °C. Anal. Calcd for $C_{16}H_{19}NO$: C, 79.63; H, 7.93. Found: C, 79.55; H, 8.01.

VCD. A solution of (−)-*erythro*-1-naphthyl-1-(2-piperidyl)-methanol, **4** (11 mg/100 μL of $CDCl_3$), was placed in a 98 μm path length BaF_2 cell. IR and VCD spectra were recorded in the 2000−900 cm^{-1} region on a modified Chiral*ir* VCD spectrometer[10] (Biotools, Inc., Wauconda, IL) at 4 cm^{-1} resolution, with the instrument optimized at 1400 cm^{-1} and 12 h collection time for sample and solvent. IR and VCD spectra of solid **4** in Nujol oil mull and IR spectra of the solution in the hydrogen-stretching region were obtained with the same instrument. Calculations of optimized geometries and IR and VCD intensities were obtained at the DFT (B3LYP functional/6-31G* basis set) level with Gaussian 98,[11] which utilizes the magnetic field perturbation method[12] with gauge-invariant atomic orbitals.[13] Calculations were carried out on the HP Superdome Complex at the University of Kentucky. Calculated frequencies were scaled by 0.97, and calculated intensities were converted into Lorentzian bands with 6 cm^{-1} half-width for comparison to experiment.

Acknowledgment. We are grateful to the following sponsors: [France] Region Alsace and CNRS to C.M. (BDI), Ministère de la Recherche to K.A. (MNERT), Ministère des Affaires Etrangères to M.R. (Co-tutelle franco-croate, No. 19981812), [USA] National Science Foundation (Grant No. CHE-0111402), National Institutes of Health (Grant No. GM63148), National Computational Science Alliance (to T.B.F.), utilizing the University of Kentucky HP Superdome Complex.

Supporting Information Available: ^{1}H NMR and ^{13}C NMR spectra for **8**, **4I** and **4II**. Calculated energies and geometries for the 10 conformers. This material is available free of charge via the Internet at http://pubs.acs.org.

JO0345502